Biophysical Journal Volume 92 January 2007 517–524

Self-Induced Docking Site of a Deeply Embedded Peripheral Membrane Protein

Simon Jaud,* Douglas J. Tobias,* Joseph J. Falke,† and Stephen H. White‡
*Department of Chemistry, and ‡Department of Physiology and Biophysics, University of California, Irvine, California; and
†Molecular Biophysics Program and The Department of Chemistry and Biochemistry, University of Colorado, Boulder, Colorado

ABSTRACT As a first step toward understanding the principles of the targeting of C2 domains to membranes, we have carried out a molecular dynamics simulation of the C2 domain of cytosolic phospholipase A2 (cPLA2-C2) in a 1-palmitoyl-2-oleoyl-phosphatidylcholine bilayer at constant pressure and temperature (NPT, 300 K and 1 atm). Using the high-resolution crystal structure of cPLA2-C2 as a starting point, we embedded two copies of the C2 domain into a preequilibrated membrane at the depth and orientation previously defined by electron paramagnetic resonance (EPR). Noting that in the membrane-bound state the three calcium binding loops are complexed to two calcium ions, we initially restrained the calcium ions at the membrane depth determined by EPR. But the depth and orientation of the domains remained within EPR experimental errors when the restraints were later removed. We find that the thermally disordered, chemically heterogeneous interfacial zones of phosphatidylcholine bilayers allow local lipid remodeling to produce a nearly perfect match to the shape and polarity of the C2 domain, thereby enabling the C2 domain to assemble and optimize its own lipid docking site. The result is a cuplike docking site with a hydrophobic bottom and hydrophilic rim. Contrary to expectations, we did not find direct interactions between the protein-bound calcium ions and lipid headgroups, which were sterically excluded from the calcium binding cleft. Rather, the lipid phosphate groups provided outer-sphere calcium coordination through intervening water molecules. These results show that the combined use of high-resolution protein structures, EPR measurements, and molecular dynamics simulations provides a general approach for analyzing the molecular interactions between membrane-docked proteins and lipid bilayers.

INTRODUCTION

Cytosolic phospholipase A2 (cPLA2) is an 85-kDa enzyme that initiates the synthesis of leukotrienes and prostaglandin, important mediators of inflammation (1–3). It consists of two domains, both structurally and functionally independent, separated by a flexible linker. The 121-residue C2 domain (cPLA2-C2) docks to phosphatidylcholine-rich intracellular membranes in response to a second messenger calcium signal (1–3) to establish membrane proximity of the 600-residue catalytic domain (Fig. 1 *a*), which hydrolytically liberates arachidonic acid from zwitterionic phospholipids after docking (1–3). Widespread in eukaryotic signaling pathways, C2 domains exhibit two conserved architectural features: an eight-strand antiparallel β-sandwich, and three negatively charged calcium-binding loops (CBLs) that typically bind two or three calcium ions and drive membrane docking (4–8). Despite these similarities, C2 motifs possess low sequence identity and target different intracellular membranes. Although crystal (9) and solution (10) structures of the cPLA2-C2 domain and a crystal structure of the entire cPLA2 protein (3) have been determined, little is known about the interactions of the cPLA2-C2 domain with membranes at the atomic level. To gain insights into these interactions, we have carried out molecular dynamics (MD) simulations of cPLA2-C2 domains docked to lipid bilayers.

The high-resolution structures show that the CBLs of cPLA2-C2, which provide multiple aspartate and asparagine side chains for the coordination of two calcium ions, are tipped with hydrophobic residues. Mechanistic studies (11,12) have shown that hydrophobic interactions, presumably involving these residues, are important in the docking of cPLA-C2 into phosphatidylcholine-rich target membranes. More generally, comparisons of different C2 domains suggest specialized membrane docking mechanisms that are dominated by electrostatic interactions in some cases, and hydrophobic interactions in others (12). This wide range of mechanisms underscores the central role of specialized protein–lipid interactions in the targeting of C2 domains to different intracellular membrane surfaces, as required by their different cellular functions. However, the molecular origins of these specialized interactions are poorly characterized, because high-resolution structures of membrane-embedded proteins and the surrounding, thermally disordered lipids cannot be obtained. Understanding the molecular interactions between the membrane-bound cPLA2-C2 and the surrounding lipids is essential for elucidating the general principles by which C2 domains stably associate with specific target membranes.

Several groups have investigated the depth and orientation of the membrane-bound cPLA2-C2 domain using fluorescence (13), NMR (10), and electron paramagnetic resonance (EPR) (14–16) methods. Each of these studies has concluded that the CBLs dominate contacts with the membrane, as predicted by the mechanistic studies. Several of these studies

Submitted June 6, 2006, and accepted for publication October 5, 2006.

Address reprint requests to Stephen H. White, University of California at Irvine, Dept. of Physiology and Biophysics, Med. Sci. I–D346, Irvine, CA 92697-4560. E-mail: stephen.white@uci.edu.

0006-3495/07/01/517/08 $2.00

doi: 10.1529/biophysj.106.090704

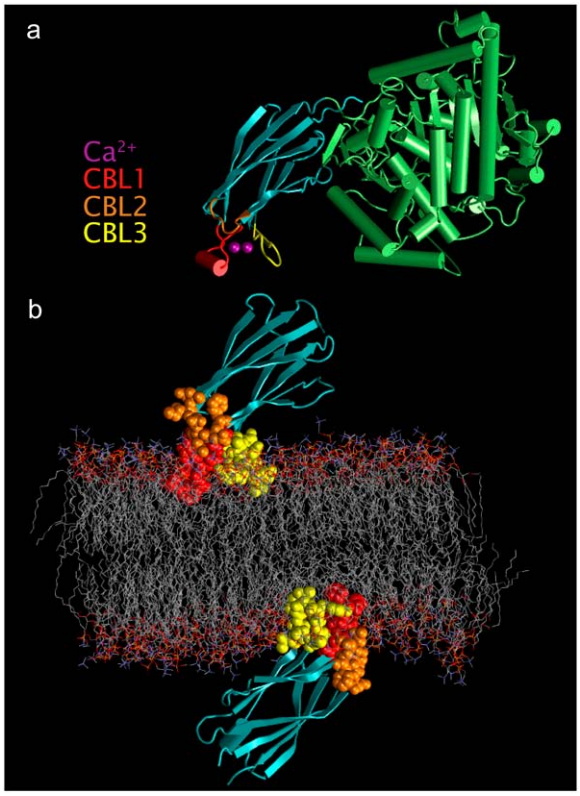

FIGURE 1 Cytosolic phospholipase A2 (cPLA2) and the interactions of its C2 domain with a POPC bilayer. (*a*) The complete cPLA2 molecule (3) (PDB 1CJY), with the C2 domain shown in blue and the catalytic domain in green. The Ca^{2+} ions are colored purple. The three Ca^{2+} binding loops (*CBL*) numbered 1, 2, and 3 are colored red, orange, and yellow, respectively. (*b*) The simulated system, in which two isolated cPLA2 C2 domains (9) (PDB 1RLW) are embedded in opposite sides of a POPC bilayer, and positioned using electron paramagnetic resonance data (16).

also propose that the two calcium ions bound by the CBLs are directly coordinated by phospholipid headgroups in the membrane-docked state. The most extensive study to date is that of Malmberg et al. (16), who used EPR measurements along with the crystal structure of the calcium-occupied cPLA2-C2 domain (9) to define the depth and orientation of the membrane-inserted domain relative to the bilayer surface. Their study examined EPR spin labels at 24 different C2 domain positions (16). Nine positions, all on the CBLs, were observed to penetrate significantly into the membrane, whereas the other 15 positions were located in or near the aqueous phase. Distance constraints determined for the membrane-embedded positions defined the depth of the domain in the bilayer and yielded angular orientations of the β-strands relative to the membrane surface.

Recent x-ray reflectivity studies (17) yielded a similar depth of the domain in the bilayer, although the data were consistent with several possible orientations of the domain relative to the membrane surface. One of these orientations closely matches the EPR-derived geometry, and the EPR data disfavor the other orientations. The published model that differs most from the EPR-derived geometry is one based on NMR chemical shift studies of cPLA2-C2 bound to dodecylphosphocholine (DPPC) micelles (10). This model, which supplements the NMR data with structural analysis of other choline-binding proteins, proposes that the bound calcium ions of the C2 domain are directly coordinated by the PC headgroup, as in the calcium-bridge model (6).

Despite these extensive previous studies, our understanding of the molecular interactions between membrane-embedded C2 domains and the surrounding lipid molecules remains incomplete. An important issue is that the membrane models used in the previous studies are static, low-resolution slab models that cannot provide any information about the specific nature of the critical lipid-protein interactions. Thus, to obtain the atomic, dynamic details of these interactions, we have carried out all-atom, dynamic computer simulations based upon the EPR membrane depth measurements (16) and the crystal structure (9) of cPLA2-C2.

Setup and technical details of the simulation

MD simulations used in concert with experimental data can, in principle, provide information about the structures and motions of the lipids surrounding a membrane-embedded protein. We considered the possibility of using the solution NMR structure (10) as the starting structure for the simulations, but we found that the conformations of the CBLs differ significantly from those of the crystal structure. We ultimately chose the crystal structure (PDB 1RLW (9)), because its CBLs are properly constrained by their native calcium coordination bonds (such bonds are invisible to NMR), its resolution is higher, and the EPR membrane-docking model was developed using the 1RLW structure. Hence, we carried out MD simulations of cPLA2-C2 docked to a lipid bilayer in the geometry specified by the EPR model (16), which was generated by studies of the native protein-bilayer complex by means of a large number of experimental distance constraints. Using the membrane depth and geometry obtained from these constraints, we embedded the crystal coordinates of the cPLA2 C2 into a bilayer made of pure 1-palmitoyl-2-oleoyl-phosphatidylcholine (POPC), which was chosen because of this domain's strong preference for PC-rich membranes (12).

We built the system from a previously hydrated and equilibrated POPC bilayer. To improve statistics and to prevent asymmetric distortions of the bilayer, we inserted a cPLA2-C2 domain into each bilayer leaflet (Fig. 1 *b*), which required removal of twenty-two overlapping lipids. The volume of the simulation cell was $\sim 90 \times 90 \times 125$ Å^3, containing 266 lipids, four calcium ions, eight chloride counter ions (to make the system electroneutral), two proteins of 121 residues each, and 19,492 water molecules, for a total of 98,110 atoms. We positioned the two domains in an offset fashion to avoid inadvertent interactions with each

other as a result of their direct proximity and the periodic boundary conditions used in the simulations. Fig. 2 reveals the lack of significant cross-bilayer overlap. The initial placement positioned the calcium ions at the level of the phosphate groups, whereas CBL1 and CBL3, which possess the most apolar side chains, were in contact with both the headgroup and hydrocarbon core regions of the membrane.

The system was set up and relaxed through a methodology comparable to that described previously (18), with one important exception: strong harmonic constraints (100 kcal/mol) were constantly applied on the position of the calcium ions throughout the production run to assure that the proteins did not stray from the experimental results. We removed these constraints at the end of the production run to verify that the system parameters remained stable and within the experimentally observed values, which was the case (Fig. 3). After protein insertion into the bilayer, a 5-ns equilibration and a 9-ns production run were performed with periodic boundary conditions using a multiple time step integrator (19,20) with an elementary time step of 1 fs. Nonbonded and electrostatic interactions were calculated every two and four time steps, respectively, with a cutoff of 11 Å. The SHAKE algorithm (21) was used to constrain the lengths of bonds involving hydrogen atoms. The particle mesh Ewald summation (22) was employed in the calculation of Coulomb interactions. The temperature was kept constant using Langevin dynamics, and a Nose-Hoover Langevin piston (23,24) was employed for pressure control (NPT, 1 bar and 300 K). The MD simulation was performed with the NAMD program (25) using the CHARMM22 protein force field (26) and CHARMM 27 lipid force field (27).

During the simulation, backbone structures of the membrane-embedded CBLs exhibited only small fluctuations away from their crystal structure conformations (Fig. 4, *a*

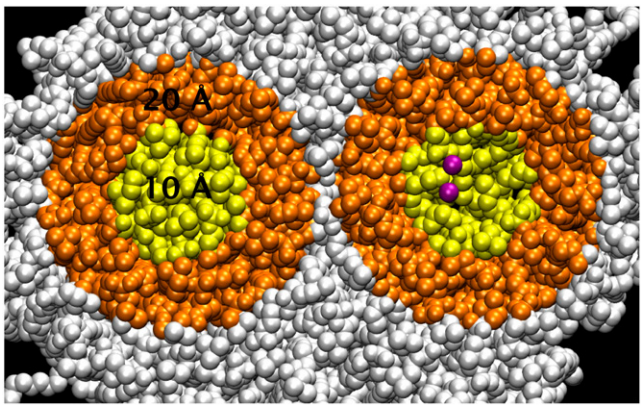

FIGURE 2 Lipids within 10 and 20 Å of the center-of-masses (COM) of the CBLs on the two bilayer surfaces, indicated by yellow and orange coloring, respectively. The two calcium ions on the membrane surface facing the viewer are shown in purple. There is no significant overlap of the C2 domains or their associated lipids across the bilayer, confirmed by an examination of the lipid order parameters in the vicinities of the two domains (Fig. 6).

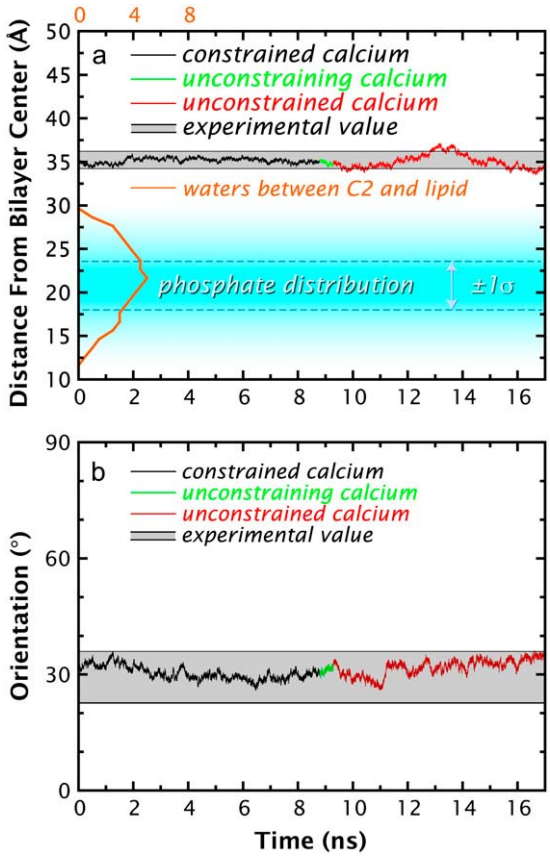

FIGURE 3 Average time-dependent COM (*a*) and orientation (*b*) of the C2 domains. The ''constrained run'' curves indicate that the constraints on the calcium ions successfully restrained the C2 domains to be within experimental uncertainties during the production run. At the end of the run, we released the constraints to ensure that they were not forcing the domains to be into a dramatically unfavorable state. After 8 ns of unconstrained simulations, the fluctuations of the COM and the orientation increase, as expected, but remain within experimental uncertainties. This indicates that the constraints on the calcium ions had no undesirable effect on the system. (*a*) The gray zones correspond to the experimental values and their experimental uncertainties. Malmberg et al. (16) calculated the C2 domain insertion depth with respect to the phosphate plane, representing the average depth of the headgroup phosphorous atom. The apparent experimental uncertainty of the depth was taken directly from the Malmberg et al. (16) article. In a dynamic bilayer, the thermally disordered phosphate groups exhibit a normal distribution along the transmembrane axis, indicated by the fuzzy sky-blue zone. This zone shows the inherent uncertainty of the positions of the phosphorous atoms normal to the bilayer. Because of this uncertainty, we calculated the protein COM with respect to the center of the bilayer rather than with respect to the phosphate plane. The average number of waters that penetrated between the protein and lipids is plotted in orange. This penetration is limited largely to the region of the phosphates. (*b*) The protein orientation is defined as the angle between the transmembrane axis and a vector from the protein COM to the protein β-sheets COM. The vector was chosen this way because of the remarkable structural stability of its starting and ending points. The uncertainty in orientation was taken as the square root of the sum of the squares of the two orientational uncertainties provided by Malmberg et al. (16).

and *c*). By contrast, the interstrand loops that are not membrane-bound exhibited much greater flexibility and larger variations from the crystal structure (Fig. 4 *d*). In other words, the bilayer and multivalent Ca^{2+} coordination damp the movement of the CBLs. However, this damping did not prevent the side chains of the CBLs from changing orientation (Fig. 4 *b*).

Structure of the self-induced socking site

During equilibration, the bilayer underwent a remarkable self-recovery from the deeply perturbing initial placement of the motifs, and generated a cavity ~25 Å deep and 30 Å wide for each C2 domain (Fig. 5 *a*). This induced docking site has the shape of a cup with a hydrophobic basin formed from the lipid alkyl chains and a hydrophilic rim formed from lipid phosphate, choline, and carbonyl groups. Each C2 domain was able to induce its own docking site, because the bilayer acts like an agitated sea of lipids that bend, twist, and reach out to contact the domain to maximize energetically favorable interactions with protein side chains (Fig. 5 *b*). Although polar interactions are extensive, there are also numerous apolar contacts located at the tips of CBL1 and CLB3. The polar collar of the protein (G33, G36, T41, K32, and D37 of CBL1; N64 and N65 of CBL2; and N95, Y96, T101, D99, and E100 of CBL3) is in contact with polar lipid headgroup components, whereas apolar side chains (A34, F35, M38, and L39 in CBL1 and V97 and M98 of CLB3) promote nonpolar interactions in the basin of the cavity (Fig. 5 *c*). But there is also a zone in which polar and apolar lipid components are in contact with both polar and apolar side chains (N95, Y96, V97, and M98 of CBL3). The ensemble of these interactions dictates the behavior of the phospholipids around the domain (Fig. 5 *d*). The lipid alkyl chains closest to CBL1 and CBL3 literally wrap around the hydrophobic residues of these loops. But this creates a void under the domain that becomes filled by extended lipid chains from the opposing leaflet. Therefore, when compared to lipids remote from the C2 domain, the lipids next to the domain are more disordered and twisted, whereas the lipids in the opposing leaflet are more oriented and stretched.

The average conformations of the lipid alkyl chains can be described in terms of the orientational order parameters S_{CH} (Fig. 6). The distorted lipids around the periphery of the protein have lower order parameters than the average lipid in a pure lipid bilayer, whereas the extended opposing lipids from the other leaflet have higher order parameters (Fig. 5 *d*). Thus, the disturbance of the C2 domain extends across the full thickness of the bilayer in its vicinity, which would not be apparent in x-ray reflectivity measurements (17) due to the low resolution of the method. Because some lipids are less ordered and others are more ordered in the vicinity of the C2 domains, lipid order parameters calculated for the whole membrane system fall within the range observed for lipids in the pure bilayer.

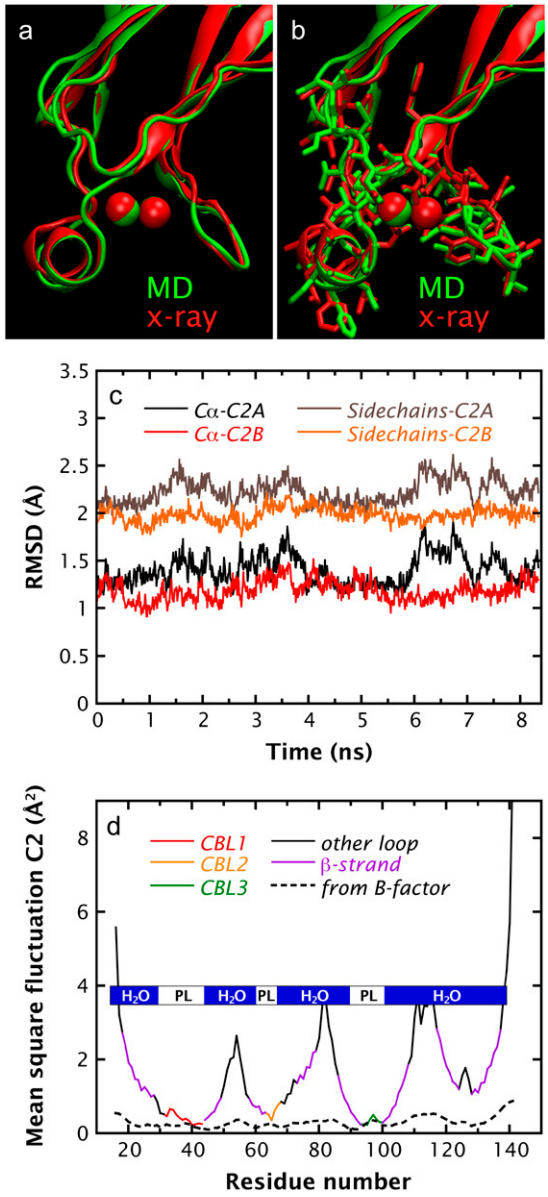

FIGURE 4 A comparison of the MD simulation structure with x-ray structure of the CBLs (*a, b*), including the root-mean-squared deviation (RMSD) of the MD structure versus the crystal structure (PDB 1RLW) of cPLA2-C2 (*c*), and an analysis of fluctuations. (*a*) RMSD of the mean MD backbone vs. crystal structure. The backbone overlap between the MD and x-ray structures is excellent (0.7 Å). The calcium ions are shown in van der Waals representation. (*b*) Side chain superimposition of the mean MD and x-ray structures. Side chains in the MD simulation reorient somewhat relative to the starting x-ray structure (1.5 Å). (*c*) Time-dependent RMSD analysis for the α-carbons and side chains of the two individual C2-domains. Domain B (*C2B*) is slightly closer to the crystal structure than domain A (*C2A*), but both domain structures are very similar. (*d*) Mean-square fluctuations at 1-ns intervals of the α-carbon backbone of the domain, along with the fluctuation calculated from the temperature factor ($B/8\pi^2$) included in the PDB file of the crystal structure. The label ''other loop'' refers to interstrand loops other than CBLs 1–3 that are typically not membrane-bound. The label ''β-strand'' refers to atoms within any of the eight β-strands. The blue- and white-striped bands indicate whether a domain region is membrane-bound (*PL*) or in water (H_2O). CBLs are not only less mobile than the β-sheets, but their rigidity is also nearly crystalline, which is explained by the damping effect of the bilayer.

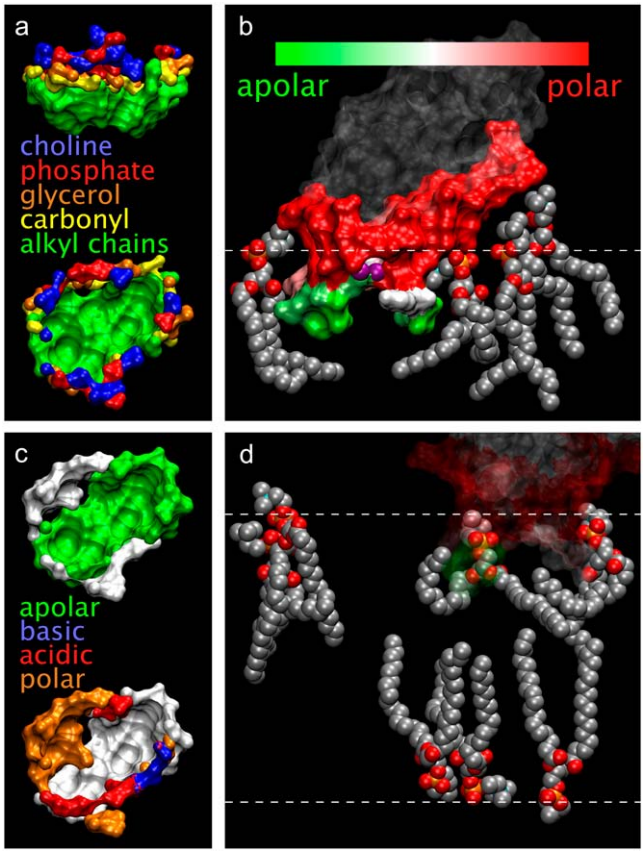

FIGURE 5 Close-up view of a C2 domain, the surrounding lipids, and a docking site. The molecular graphics images were prepared using the VMD program (30). (*a*) Top and side views of the docking site organized by the CBLs, color-coded for the different lipid subgroups constituting it. (*b*) Surface representation of a domain, showing a few representative lipids wrapping and extending around it. The color coding of the domain shows the time-averaged type of contact with the lipids within 4 Å, whereas transparent regions represent contacts with water only. The dashed line indicates the mean position of the phosphate groups. (*c*) Two top views of the docking site (shown as a white surface) on which is superimposed the types of interactions (shown by color coding) that each makes with nearby protein residues (within 6 Å). (*d*) Different classes of lipids found in the system: distant lipids (*far left*) never interact with the domain whereas lipids next to the CBLs are twisted and disordered, creating a void under the domain. The lipids opposite to the domain have moved into this void by becoming more extended and ordered.

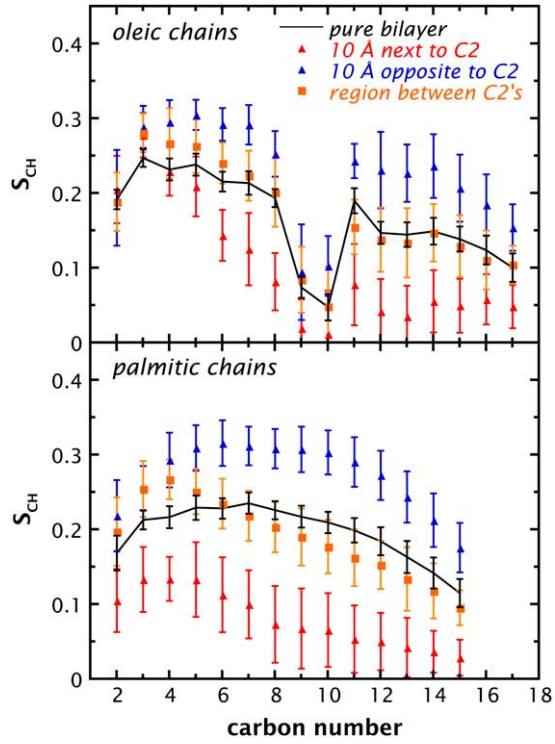

FIGURE 6 Orientational order parameters S_{CH} of the palmitic and oleic chains of POPC in pure bilayers and in the vicinity of the C2 domains. Here the order parameter is $S_{CH} = \frac{1}{2}\langle 3\cos^2\theta - 1\rangle$, where θ is the angle that a C–H bond makes with respect to the bilayer normal. The error bars represent the standard deviations of the data obtained from block averages (31) over 1-ns intervals. A high order parameter is indicative of more extended, oriented alkyl chains, whereas a low value represents nonlinear, disordered chains. The pure bilayer data were obtained from a simulation containing 864 lipids and no protein. The labels ''10 Å next to C2'' and ''10 Å opposite to C2'' refer to a transmembrane cylinder of lipids located within 10 Å of the (x,y)-coordinates of the center of mass of the CBLs, on the leaflet adjacent and opposite to the domain, respectively. The label ''region between C2's'' refers to a transmembrane cylinder of lipids located on the membrane plane, between the two domains (Fig. 2). This cylinder has a radius of 10 Å and does not overlap with the ''10 Å next to C2'' and ''10 Å opposite to C2'' regions. In this region, the data overlap with the data for the pure bilayer. This confirms that the two domains were embedded sufficiently far from each other to avoid perturbing the whole region between them.

To quantify the interactions underlying this behavior, the average numbers of contacts between each CBL residue and the headgroup components (choline, phosphate, glycerol, carbonyl, alkyl chains) were calculated (Fig. 7 *a*). The results confirm the high density of apolar contacts at the tips of CBL1 and CBL3 (Fig. 7 *b*), and reveal that lipid hydrocarbon chains interact solely with CBL1 and CBL3, where they cluster around F35 and V97, while avoiding close interactions with charged residues. The carbonyl contacts are very similar to those of the alkyl chains but show a weak preference for CBL3. The glycerols exhibit the fewest contacts, and are distributed with remarkable evenness among all three CBLs. Because CBL2 lacks the hydrophobic residues of CBL1 and CBL3, most of the lipid contacts with CBL2 involve the charged choline and phosphate moieties. In addition, the positively charged cholines exhibit an important distribution centered around the acidic residues D99 and E100 on CBL3. Despite their negative charge, phosphates also exhibit an important concentration around CBL3, in some cases because their positions are correlated with the cholines. The phosphates also exhibit a significant presence near the basic K32 and near one of the positively charged calcium ions.

Our results also show that the bilayer plays a central role in the docking process by adapting its shape and polarity to the topology of the domain, to accommodate charged, polar, and apolar groups. For instance, the phosphate group that provides

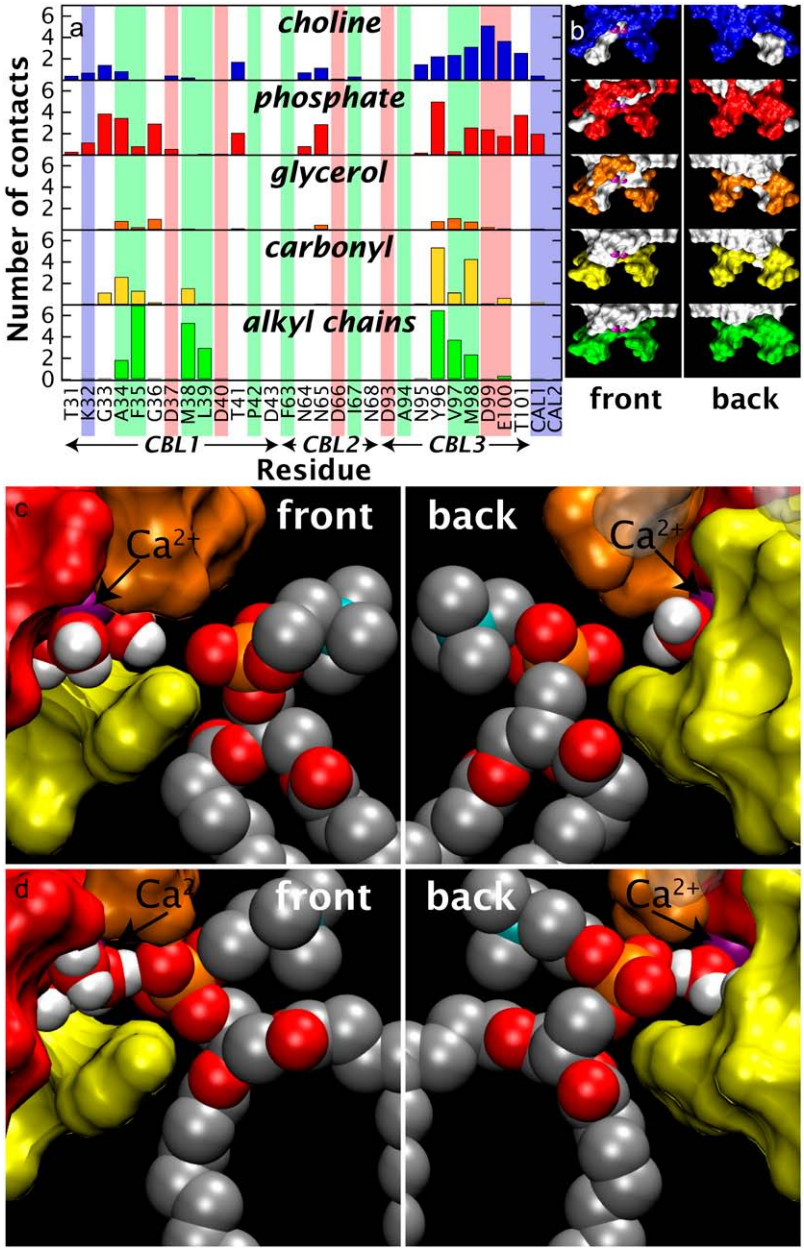

FIGURE 7 The contacts between the C2 domains and the lipids, and the CBL cage protecting the calcium ions. (*a*) Time-averaged number of contacts between the CBL residues and the lipids within 4 Å, color-coded by lipid subgroups, and within 6 Å for the calcium ions. The transparent vertical bars correspond to types of interaction: positively charged groups (*blue*), negatively charged groups (*red*), apolar residues (*green*), and polar residues (*white*). (*b*) Front and back views of the CBLs illustrating the location of the contacts on their surface, color-coded by lipid subgroups. The apolar interactions are limited to the tip of the CBLs, whereas the polar interactions are less selective. (*c*) Front and back views of the three CBLs and the three water molecules shielding the Ca^{2+} ions from PC. The lipid cannot reach the calcium because it is sterically hindered by the CBLs. (*d*) Same as panel *c*, but for the unrestrained system. Given the thermal motion of the system, there is no significant difference between panels *c* and *d*.

outer sphere calcium coordination had to move into the proximity of the calcium binding cleft to act as a counter-ion, as observed in previous work (18). Similarly, lipid acyl chains moved to solvate the hydrophobic side chains of CBLs 1 and 3 embedded in the apolar bilayer core. Water moves freely within the region of the CBLs where the calcium ions are located, penetrating into the bilayer to within 12 Å of the bilayer center (Fig. 3 *a*).

Calcium coordination

In the calcium bridge model (6,10), C2-domain docking is stabilized by simultaneous coordination of the calcium ions by both protein and phospholipid headgroup oxygens. But that is not observed in the simulation. Instead of direct calcium coordination with lipid phosphates, we found indirect coordination mediated by intervening water molecules (Fig. 7 *c*). Calcium is thus directly coordinated only by protein and water oxygens, as in the crystal structure of the free complex. The simulation clearly shows that the headgroup phosphates are unable to coordinate calcium directly, because the lipids are too bulky to infiltrate the CBL calcium-binding cage. Releasing the restraints on the calcium ions allowed these ions and the headgroup phosphates to move within the range made available by thermal motion, but the phosphates never penetrated into the inner coordination shell of the calcium

ions (Fig. 7 *d*). This is in contrast to the previous NMR-derived model (10), which predicted that there was sufficient space to fit glycerophosphocholine (GPC), a PC headgroup analog, between the CBLs. But this PC headgroup analog is much shorter than a typical phospholipid, because it lacks long alkyl chains. This, and the fact that the calcium ions are farther apart in the solution NMR structure (5.6 Å) than in the crystal structure (4.2 Å), might explain why it was possible to introduce GPC between the CBLs in the NMR model.

The observation that the calcium ions are not directly coordinated by lipid headgroups strongly supports the electrostatic switch model of Murray and Honig (28) for the calcium activation of cPLA2-C2 membrane docking. These authors have demonstrated through electrostatic calculations that the neighborhood of the calcium-free CBLs is strongly negatively charged, which would prevent docking to the membrane surface. Upon calcium binding, the CBLs become overall neutral, thereby allowing membrane docking and penetration into the bilayer core. In the simplest version of this model, the calcium ions serve only as an electrostatic switch and do not directly interact with lipid headgroups to stabilize the membrane docking, as observed in the simulation.

CONCLUSIONS

Structural studies of pure bilayers carried out by combined x-ray and neutron diffraction have revealed that the 15-Å-thick interfacial zones of lipid bilayers, dominated by the phospholipid headgroups, are highly dynamic regions of tumultuous chemical heterogeneity (29). This remarkable property allows the lipids to reorganize themselves easily in the vicinity of embedded proteins to optimize the interactions between protein and lipid, creating in this case a cavity in the lipid bilayer that mirrors the properties of the C2 domain. We suggest that this idea underlies the targeting and membrane docking of C2 domains, and of peripheral membrane proteins in general. Each type of conserved C2 domain likely requires specific lipids, or mixtures of lipids, and a specific penetration depth to create the optimal complementary contacts between the protein surface and the targeted membrane. Our results show that these important details of targeted docking can be obtained from MD simulations used in concert with crystallographic and EPR data. But this is only a beginning; several other types of C2-domain must be studied before their targeting can be fully understood in terms of protein-lipid interactions. Future simulations must examine the importance of mixtures of lipids—particularly cholesterol—in determining bilayer fluidity, adaptability, and protein specificity of the interfacial region. An interesting question that demands closer attention is whether the transbilayer influence of the C2 domains on the opposing bilayer leaflet will be a persistent finding, independent of lipid composition.

We thank Dr. Alfredo Freites for supplying the trajectory of the neat lipid bilayer.

This research was supported by grants from the National Institute of General Medical Sciences to S.H.W. and J.J.F., from the National Center for Research Resources to S.H.W., and from the National Science Foundation to D.J.T. ''Le Fond Québecois de la Recherche sur la Nature et les Technologies'' provided a graduate fellowship for S.J.

REFERENCES

1. Leslie, C. C. 2004. Regulation of the specific release of arachidonic acid by cytosolic phospholipase A2. *Prostaglandins Leukot. Essent. Fatty Acids.* 70:373–376.
2. Clark, J. D., A. R. Schievella, E. A. Nalefski, and L.-L. Lin. 1995. Cytosolic phospholipase A2. *J. Lipid Mediat. Cell Signal.* 12:83–117.
3. Dessen, A., J. Tang, H. Schmidt, M. Stahl, J. D. Clark, J. Seehra, and W. S. Somers. 1999. Crystal structure of human cytosolic phospholipase A2 reveals a novel topology and catalytic mechanism. *Cell.* 97:349–360.
4. Cho, W., and R. V. Stahelin. 2005. Membrane-protein interactions in cell signaling and membrane trafficking. *Annu. Rev. Biophys. Biomol. Struct.* 34:119–151.
5. Bai, J., and E. R. Chapman. 2004. The C2 domains of synaptotagmin—partners in exocytosis. *Trends Biochem. Sci.* 29:143–151.
6. Hurley, J. H., and S. Misra. 2000. Signaling and subcellular targeting by membrane-binding domains. *Annu. Rev. Biophys. Biomol. Struct.* 29:49–79.
7. Rizo, J., and T. C. Südhof. 1998. C2-domains, structure and function of a universal Ca2+-binding domain. *J. Biol. Chem.* 273:15879–15882.
8. Nalefski, E. A., M. M. Slazas, and J. J. Falke. 1997. Ca2+-signaling cycle of a membrane-docking C2 domain. *Biochemistry.* 36:12011–12018.
9. Perisic, O., S. Fong, D. E. Lynch, M. Bycroft, and R. L. Williams. 1998. Crystal structure of a calcium-phospholipid binding domain from cytosolic phospholipase A2. *J. Biol. Chem.* 273:1596–1604.
10. Xu, G.-Y., T. McDonagh, H.-A. Yu, E. A. Nalefski, J. D. Clark, and D. A. Cumming. 1998. Solution structure and membrane interactions of the C2 domain of cytosolic phospholipase A_2. *J. Mol. Biol.* 280:485–500.
11. Perisic, O., H. F. Paterson, G. Mosedale, S. Lara-González, and R. L. Williams. 1999. Mapping the phospholipid-binding surface and translocation determinants of the C2 domain from cytosolic phospholipase A2. *J. Biol. Chem.* 274:14979–14987.
12. Nalefski, E. A., M. A. Wisner, J. Z. Chen, S. R. Sprang, M. Fukuda, K. Mikoshiba, and J. J. Falke. 2001. C2 domains from different Ca^{2+} signaling pathways display functional and mechanistic diversity. *Biochemistry.* 40:3089–3100.
13. Nalefski, E. A., and J. J. Falke. 1998. Location of the membrane-docking face on the Ca^{2+}-activated C2 domain of cytosoic phospholipase A2. *Biochemistry.* 37:17642–17650.
14. Frazier, A. A., M. A. Wisner, N. J. Malmberg, K. G. Victor, G. E. Fanucci, E. A. Nalefski, J. J. Falke, and D. S. Cafiso. 2002. Membrane orientation and position of the C2 domain from cPLA2 by site-directed spin labeling. *Biochemistry.* 41:6282–6292.
15. Nielsen, R. D., K. Che, M. H. Gelb, and B. H. Robinson. 2005. A ruler for determining the position of proteins in membranes. *J. Am. Chem. Soc.* 127:6430–6442.
16. Malmberg, N. J., D. R. Van Buskirk, and J. J. Falke. 2003. Membrane-docking loops of the cPLA2 C2 domain: Detailed structural analysis of the protein-membrane interface via site-directed spin-labeling. *Biochemistry.* 42:13227–13240.
17. Málková, S., F. Long, R. V. Stahelin, S. V. Pingali, D. Murray, W. Cho, and M. L. Schlossman. 2005. X-ray reflectivity studies of cPLA2α-C2 domains adsorbed onto Langmuir monolayers of SOPC. *Biophys. J.* 89:1861–1873.
18. Freites, J. A., D. J. Tobias, G. von Heijne, and S. H. White. 2005. Interface connections of a transmembrane voltage sensor. *Proc. Natl. Acad. Sci. USA.* 102:15059–15064.

19. Tuckerman, M., and B. J. Berne. 1992. Reversible multiple time scale molecular dynamics. *J. Chem. Phys.* 97:1990–2001.

20. Grubmüller, H., H. Heller, A. Windemuth, and K. Schulten. 1991. Generalized Verlet algorithm for efficient molecular dynamics simulations with long-range interactions. *Mol. Simul.* 6:121–142.

21. Ryckaert, J.-P., G. Ciccotti, and H. J. C. Berendsen. 1977. Numerical integration of the Cartesian equations of motion of a system with constraints: molecular dynamics of *n*-alkanes. *J. Comput. Phys.* 23:327–341.

22. Darden, T., D. York, and L. Pedersen. 1993. Particle mesh Ewald: An $N\cdot\log(N)$ method for Ewald sums in large systems. *J. Chem. Phys.* 98:10089–10092.

23. Martyna, G. J., D. J. Tobias, and M. L. Klein. 1994. Constant-pressure molecular-dynamics algorithms. *J. Chem. Phys.* 101:4177–4189.

24. Feller, S. E., Y. Zhang, R. W. Pastor, and B. R. Brooks. 1995. Constant pressure molecular dynamics simulation: the Langevin piston method. *J. Chem. Phys.* 103:4613–4621.

25. Kalé, L., R. Skeel, M. Bhandarkar, R. Brunner, A. Gursoy, N. Krawetz, J. Phillips, A. Shinozaki, K. Varadarajan, and K. Schulten. 1999. NAMD2: Greater scalability for parallel molecular dynamics. *J. Comput. Phys.* 151:283–312.

26. MacKerell, A. D. Jr., D. Bashford, M. Bellott, R. L. Dunbrack Jr., J. D. Evanseck, M. J. Field, S. Fischer, J. Gao, H. Guo, S. Ha, D. Joseph-McCarthy, L. Kuchnir, et al. 1998. All-atom empirical potential for molecular modeling and dynamics studies of proteins. *J. Phys. Chem. B.* 102:3586–3616.

27. Feller, S. E., and A. D. MacKerell Jr. 2000. An improved empirical potential energy function for molecular simulations of phospholipids. *J. Phys. Chem. B.* 104:7510–7515.

28. Murray, D., and B. Honig. 2002. Electrostatic control of the membrane targeting of C2 domains. *Mol. Cell.* 9:145–154.

29. Wiener, M. C., and S. H. White. 1992. Structure of a fluid dioleoylphosphatidylcholine bilayer determined by joint refinement of x-ray and neutron diffraction data. III. Complete structure. *Biophys. J.* 61:434–447.

30. Humphrey, W., W. Dalke, and K. Schulten. 1996. VMD: visual molecular dynamics. *J. Mol. Graph.* 14:33–38.

31. Flyvbjerg, H., and H. G. Petersen. 1989. Error estimates on averages of correlated data. *J. Chem. Phys.* 91:461–466.